Proceedings 10th NUMGE 2023
10th European Conference on Numerical Methods in Geotechnical Engineering
Zdravkovic L, Kontoe S, Taborda DMG, Tsiampousi A (eds)

https://doi.org/10.53243/NUMGE2023-81

Simulating dry granular flow impacts on 3D rigid obstacles

M. Kontoe[1] , S. Lopez-Querol[1] , T. Rossetto[1]

[1]*Department of Civil, Environmental and Geomatic Engineering, U.C.L., London, UK*

ABSTRACT: The scope of this study is to identify the loads acting on a 3D structure impacted by a dry granular flow using numerical modelling. The developed models deploy the Material Point Method (MPM) owing to its capability in capturing large-strain deformation problems. Initially, a 2D model of an experiment from the literature is developed. The experiment refers to a small-scale flume test which monitors the impact of a dry granular flow on a rigid obstacle with different inclinations of the flume. The developed numerical model accurately replicates a previously validated simulation, regarding the impact process and obtained measurements and therefore, captures efficiently the experimental response. The 2D numerical model is then extended to a 3D computational domain, indicating sensitivity of the impact force records upon the assigned number of material points representing the granular flow. The calibrated 3D model is modified to consider reduced obstacle width, to capture the variability of induced soil pressure on the structures and simulate the soil flow when surrounding them. The implemented modifications indicate a degrading post-peak branch linked to the decreasing sediment at the front face of the structure.

Keywords: MPM; Dry granular flow; Impact force; Reduced width obstacle; Flume experiment

1 INTRODUCTION

Landslides represent the 4th most frequent hazard, according to the International Disaster Database EM-DAT (D. Guha-Sapir et al., 2008), resulting in disastrous consequences to the affected communities and building stock. Between 1900 and 2014, the EM-DAT reports almost 65000 casualties and 13.7 billion people affected due to landslides worldwide, while it estimates 8.7 billion USD of financial loss (Parisi & Sabella, 2017). The numbers could be even underestimated due to landslides being treated as secondary hazards.

Reinforced concrete rigid barriers are among the most widely implemented strategies towards mitigating the consequences of large fast-moving debris flows (Kwan, 2012). There is intensive research focused on understanding the impact mechanism of soil flows (debris flows, dry and saturated granular flows), as well as quantifying the magnitude and distribution of the induced earth pressures on protection structures, to determine the vulnerability and suggest guidelines for the safe design of these elements (e.g. Jiang & Towhata, 2013; Scheidl et al., 2013). Only a few relevant publications rely on obtaining data from field observations and full-scale experiments. Scheidl et al. (2013) comment that the cost of monitoring equipment required for these studies, in addition to the unknown frequency of the landslides‘ occurrence and lack of relevant information about the soil properties on-site, led many authors to focus on performing small-scale experiments (e.g. Moriguchi et al., 2009; Ng et al., 2017). However, miniaturised tests involve challenges in capturing field-phenomena due to scaling effects (Iverson, 1997). To address the scaling considerations, researchers often employ dimensional analysis to ensure consistent response of soil flows across different scales. Macroscopic dimensional analysis is the most commonly implemented approach, which involves interpreting the experimental earth pressures to estimate actual landslide forces, provided that the Froude (Fr) number on site falls within the range achieved in the tests. The application of the Fr law to adjust the response of laboratory tests to mimic upscaled conditions is limited to a small reach that contains the obstacle (Zanuttigh & Lamberti, 2006).

Numerical models, validated upon published experiments, are also deployed in the literature, to simulate the soil to obstacle interaction. The Material Points Method (e.g. Cuomo et al., 2021; Nakajima et al., 2019), and the Discrete Element Method (e.g. Shen et al., 2018), are the most commonly employed approaches. Other studies implement alternative numerical schemes such as the Eulerian method (Moriguchi et al., 2009).

The experimental and numerical results indicate two mechanisms describing the soil impact to the rigid obstacle, the pile-up and run-up, encountered in dry and partially to fully saturated granular flows respectively (Ng et al., 2017). In dry granular flows, specifically, past studies report the formation of a static zone immediately after the first impact. The incoming soil overtops with reduced dynamics the initial deposit, generating additional sediment, eventually reaching a maximum height. Then, the incoming material deposits at the rear section of the static zone. The interaction between the static zone and the incoming soil contributes

significantly in the energy dissipation of the flow, shielding the obstacle (Ng et al., 2017; Shen et al., 2018). Koo et al. (2017) suggest also that the material overtopping the static zone partially bounces back reducing the velocity of the incoming soil flow. The authors highlight the barrier's efficiency in transforming kinetic to potential energy of the soil flow, expressed, in their experiments, as reduced velocity and depth of the granular flow in the presence of the obstacle. An additional factor contributing to the energy dissipation of the flow is the angle of the obstacle with respect to the horizontal level. Shen et al. (2018), perform multiple simulations, accounting for different angles of the obstacle. For less steep barriers, the impact force is reduced owing to the convex shape of the deposits which allows for increased run-out distance.

The measured normal pressure at the face of the barrier shows an initial steep increase reaching a peak value, which then, gradually reduces to a residual force. Scheidl et al., 2013 observe that the peak occurs almost simultaneously with the first impact. Moriguchi et al. (2009) report that the impact forces consist of the dynamic and static force components. The governing component in the peak impact alternates upon the velocity of the dry granular flow, while the residual coincides with the applied static load. Likewise, Jiang & Towhata (2013) observe the dominancy of the static over the dynamic force as the velocity of the incoming granular material progressively decreases.

The review of the available publications reveals considerable ongoing investigation on the interaction between soil flows and full-spanning width obstacles. However, there are limited efforts in determining the impact mechanism on obstacles with different geometries. Zanuttigh & Lamberti (2006) performed small-scale experiments on rigid structures of various types and observe their subsequent effect on the obtained forces. The primary objective of this study is to conduct a numerical investigation into the impact mechanism on obstacles with reduced width. This is accomplished by modifying the geometry of the retaining element within a simulation firstly validated against experimental data from the literature.

2 METHODOLOGY

2.1 Case Study Description

The numerical model developed for this study simulates the small-scale flume experiments, performed by Moriguchi et al. (2009). The authors focused on investigating the effect of the flume's inclination on the induced impact forces from a granular flow to a rigid obstacle. The configuration of the experimental flume is illustrated in Figure 1. The inclination of the flume was varied to achieve angles of 45, 50, 55, 60 and 65 degrees. The authors placed a box filled with dry Toyoura sand, of 50kg weight, at the top of the flume. In the experiments, the door of the box opened instantly allowing the granular material to flow and impact an obstacle, of 0.3m height, located at the end of the flume. The forces were measured with a load cell attached to the rigid wall. The bottom of the flume was coated with the sand to generate friction between the granular flow and the apparatus, while the contact between the soil and the wall was perceived as smooth. Five experimental trials, for each of the flume's configurations, were conducted. The authors observed that the magnitude of the recorded peak impact forces increases significantly with increasing flume angles.

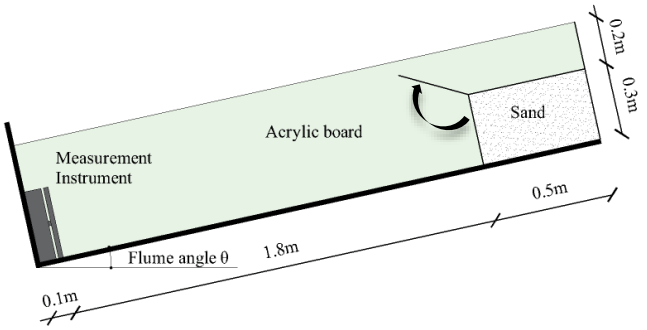

Figure 1: Experimental setup, after Moriguchi et al. (2009)

2.2 Numerical Modelling

The numerical models developed in this study adopt the MPM approach (Sulsky et al., 1994), as integrated within the Anura3D software. Soga et al. (2016) conducted a comprehensive review of the available numerical techniques for simulating landslides, including the Discrete Element Method (DEM), the Smooth-Particle Hydrodynamics (SPH), the Particle Finite Element Method (PFEM) etc. and highlighted the accuracy of MPM in capturing complex failure mechanisms and the interaction between the solid and fluid phases of the medium. MPM has been successfully deployed in previous studies to simulate documented landslides as well as, laboratory experiments on soil flows and miniaturized slopes.

This study initially develops a 2D simulation of the experiment described in section 2.1, adhering to the numerical assumptions proposed by Cuomo et al. (2021), who calibrated their MPM model upon the same test. The objective of replicating this 2D model is to validate the current simulation and establish a reliable foundation for subsequent modifications. Hence, the material properties, the contact response characteristics, and the mesh size deployed in the simulation are consistent with the reference numerical study. Additional parameters as the number of material points per cell and the applied local damping factor are adjusted accordingly to achieve comparable results.

The experiment is modelled horizontally while the variability in the flume angle is considered via modifying the gravity vector accordingly. The boundaries of the computational domain extend to accommodate the

potential soil overflowing downstream of the obstacle, reported by Cuomo et al. (2021). The granular material and the flume apparatus as well as the obstacle are modelled via the Mohr-Coulomb and Elastic constitutive laws respectively. The prescribed material properties are summarised in Table 1. Similarly to Cuomo et al. (2021), the frictional contact between the soil and the flume base is assigned equal to 40°, while the interaction between the soil and the obstacle is modelled as smooth.

Table 1: Material properties after Cuomo et al. (2021)

Material	ρ_s *(kg/m³)*	n	E *(MPa)*	c *(kPa)*	φ (°)	ψ (°)
Dry sand	2650	0.48	20	0	40	0
Obstacle	7850	0	∞	-	-	-
Flume	7850	0	∞	-	-	-

The size of the triangular elements deployed for the background mesh of the 2D model is equal to 0.02m. The number of integration points adopted per cell is preliminary tested assuming 1 and 3MPs per cell representing the soil box, to identify the optimum configuration. The results demonstrate that adopting 3 MPs per element contributes to reproducing comparable magnitude and evolution of impact forces with Cuomo et al. (2021). In addition, it ensures simulating consistent granular flow profile with the calibrated model. To limit the computational cost of the analysis the rigid elements are represented by the minimum number of MPs, i.e. one, since the integration points are not expected to move among adjacent cells.

The top and lateral sides of the computational domain are restrained accordingly to limit the movement of the MPs outside the computational domain. To reflect the experimental conditions, the simulations are initially subjected to gravity analysis while preventing the lateral deformation of the granular material. Subsequently, dynamic analysis is performed to capture the response of the flow while removing the applied constraints to the soil mass. To reproduce the duration of the experiment, i.e. 2sec, the models are analysed in 20 load-steps with a time increment of 0.1s. As recommended by Fern et al. (2019), a local damping factor of 0.75 and 0.05 is adopted for the gravity and dynamic analysis respectively. The coefficients accelerate the convergence in the static analysis and simulate the energy dissipation from the soil material in the dynamic analysis. To limit the impact of kinematic locking, the strain smoothening technique is employed, which improves the response of the granular flow and yields results consistent with Cuomo et al. (2021). To effectively address the cell-crossing induced oscillations in the numerical solution, the mixed MPM-Gauss computational method is deployed. Anura3D incorporates these options to tackle the instabilities commonly encountered in MPM.

By ensuring similarity between the obtained measurements with the findings of Cuomo et al. (2021), the analysis is then extended to the 3D domain, to investigate the influence of the reduced blockage ratio on the granular flow impact mechanism, while maintaining the described modelling strategy. The modulus of elasticity *(E)* for the rigid elements is calibrated to ensure numerical stability and computational efficiency. In the explicit integration scheme of MPM, in Anura3D, the critical time step is determined by the ratio between the smallest element size and the *E* (Fern et al., 2019). The maximum critical time step to achieve the stability of the numerical solution is in the order of magnitude of 10^{-5}. Given that the smallest mesh element is below 0.02m and the minimum *E* employed is 5000MPa the critical time step for the elastic analysis is equal to $1.1*10^{-5}$s. The time increment is further reduced by the Courant number which is set equal to 0.98 for the non-linear analysis. It should be noted that for simulations involving increased complexity, such as those considering the reduced blockage ratio, further adjustment of the time step may be required. The dimension of the elements along the width of the flume is investigated to evaluate their influence on the numerical results, indicating negligible sensitivity. The tested size of the tetrahedra elements is assumed equal to 0.025m, 0.05m and 0.1m while the dimension in xy plane is maintained equal to 0.02m. The developed model accounts for 4 segments with size equal to 0.025m along the section of the flume. Calibration of the 3D model assuming initially a full width obstacle is performed regarding the assigned number of material points representing the granular material within the soil box. Upon the validation of the 3D simulation, the geometry of the obstacle is modified to investigate numerically the effect of the reduced blockage ratio on the impact mechanism. The results refer to a structure of width equal to 50% of the flume. The height of the retaining element is also increased to limit the potential soil from overflowing.

Similarly to Cuomo et al. (2021), the records from all simulations are post-processed, in MATLAB, to obtain the mean trendline of the soil impact forces. The data lying outside the range of three local scaled median absolute deviations from the local median, over a defined window of records, are removed as outliers. A Gaussian curve is then, fitted while varying the number of terms to appropriately represent the trend of the data.

3 RESULTS

3.1 Validation of the 2D flume model

The 2D MPM model developed in this study is analysed for the flume angles tested in the original experiment. To assess the accuracy of the adopted modelling assumptions, the force results are compared to the findings obtained from the calibrated models of Cuomo et al. (2021), which effectively capture the experimental response. In particular, the 2D flume simulations

developed by the authors predict values of peak impact forces deviating from the experimental measurements by maximum 15%. Figure 2 demonstrates that the present analysis replicates the impact mechanism reported by Cuomo et al. (2021). The force trendlines, derived in this study, exhibit a similar pattern to relevant observations from the literature, characterised by a steep increase to the peak values followed gradually by a plateau. The first impact, the subsequent peak, and the progressive reduction to the residual forces occur simultaneously in both models, with very similar magnitudes too, although the peak impact is overestimated in the current research. The present simulations predict maximum forces that vary from 5% to 18% with respect to the values reported by Cuomo et al. (2021). This discrepancy is associated with the subjective criteria adopted in the fitting process by both studies. The amplitude of oscillations recorded during the first impact present significant fluctuation, leading to the observed differences in the maximum forces. However, the residual values are almost coincident, as towards the end of the analyses, the range of oscillations diminishes and therefore, the effect of the deployed assumptions to the fitting results is limited.

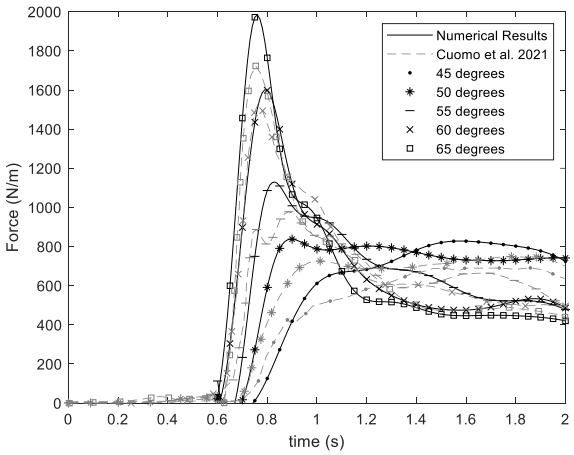

Figure 2: 2D simulation results against Cuomo et al. (2021)

The deformed shape of the granular flow obtained from the current numerical analysis, for the flume angle of 45°, is compared to the soil flow profile depicted by Cuomo et al. (2021), indicating consistency and revealing that the present model adequately captures the propagation of the soil material. To maintain brevity, this comparison is presented solely for the extended 3D model in section 3.2.

3.2 3D Numerical model

The 3D models of the experimental setup developed for this study assume a flume inclination of 45°. The performance of the simulations is tested upon the number of MPs allocated per cell, which is set at 1 and 4 to represent the soil mass. Figure 3 provides a comparison of the measured impact forces at the obstacle face, normalized by the flume width, with the experimental and numerical results from previous studies.

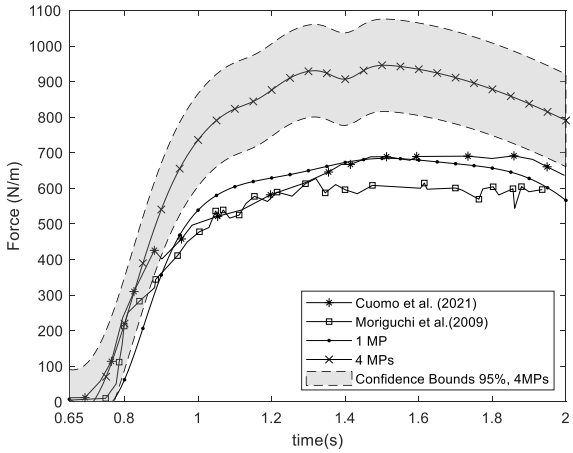

Figure 3: Comparison of Impact Forces from the 3D models with Moriguchi et al.(2009) and Cuomo et al.(2021).

The captured forces from the 3D models show an evident fluctuation upon the tested parameters, as well as with respect to the relevant observations from the literature. The variability in the obtained forces is reflected in the recorded range of magnitudes, indicating the considerable sensitivity of the numerical results to the modelling assumptions. It is evident that deploying reduced MPs within the granular flow leads to a closer simulation of the experimental and numerical results from the literature. Conversely, employing 4 MPs results in overpredicting the obtained impact with respect to the reference measurements, due to imposing overlay constraints to the system. Kinematic locking instability, which becomes more pronounced with the increased number of integration points per cell, could be effectively mitigated but not eliminated via the adopted strain-smoothening technique. However, the latter analysis (4 MPs) achieves detailed representation of the granular flow and ensures the stability of the numerical solution by addressing convergence issues. These observations are particularly interesting for the subsequent simulations involving reduced width obstacles, since the impact mechanism becomes more complex.

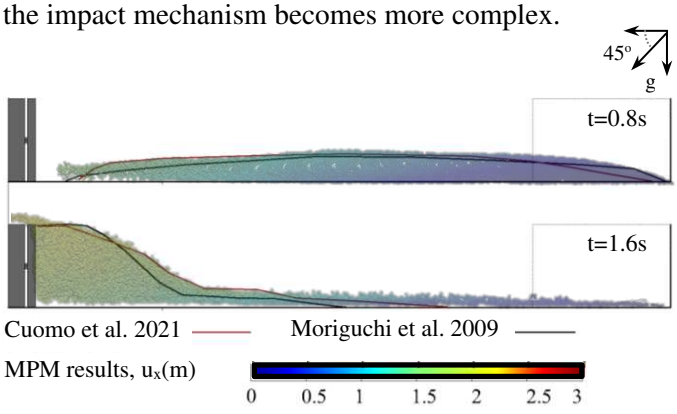

Figure 4: Comparison of the soil flow configuration

Figure 3 provides the 95% confidence bounds for the derived mean curves of the model with the 4MPs to

account for the uncertainty in the fitting process due to the considerably fluctuating measurements. The peak experimental forces reported by Moriguchi et al. (2009) for the conducted trials, ranging from 564N/m to 710N/m, fall within the identified confidence intervals ensuring the reliability of the obtained solution. To highlight the validity of the proposed modelling, Figure 4 compares the soil flow configuration at different time steps, captured via the simulation with 4MPs, and the observations from the literature, indicating that the obtained soil propagation and impact mechanisms are identical. Therefore, the simulation with 4MPs is deployed for further analysis in the next section.

3.3 Impact mechanism for reduced blockage ratio

The 3D model is modified to accommodate a reduced blockage ratio, assuming the obstacle's width equal to 0.05m (half of the flume), while initially maintaining constant height *(h=0.3m)*. The geometry of the barrier is further modified to restrict the material from overflowing, by increasing the element's height to h=0.9m.

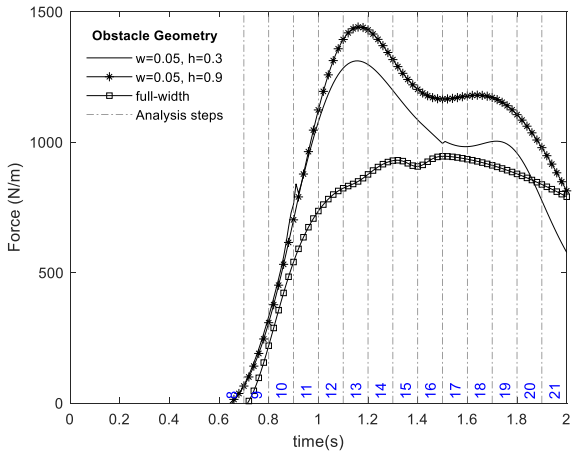

Figure 5: Recorded impact forces at the modified obstacles

Figure 5 illustrates the evolution of earth pressures measured at the front face of the obstacle, from both simulations, revealing the progress of the captured impact mechanism. The granular flow reaches the obstacle during step 9 when the first impact is recorded. In the following analysis steps the soil runs-up at the face of the obstacle across the section of the flume and discharges by developing complicated streamlines, as illustrated in Figure 6 (a). The run-up height is similar throughout the section width. The size of the obstacle is large enough to affect the response of the granular flow almost uniformly throughout the width of the model. Figure 6 (c) illustrates the section-cuts performed along the flume to observe the interaction between the soil and the obstacle.

The presence of the obstacle forces the material to deviate from its straight path and redirects the flow around the corners of the barrier as shown in Figure 6 (b). The material discharges through the sides of the obstacle via generating two pathways observed in Figure 6 (a1) & (a2). S2 indicates considerable material discharge, owing to the additional diverging soil flow from the rest of the sections to the boundary elements. The depth of the soil flow exceeds the obstacle height during step 11, only for the model which assumes h=0.3m, i.e.. Model 1, leading to the material overflowing the barrier in the subsequent steps, and providing an additional streamline. Considerable material discharge occurs from step 13 onwards, therefore, the maximum force is recorded during the step, i.e. 12. The flow-depth drops gradually in the following steps owing to the continuously reducing accumulated soil volume at the front face of the obstacle. In model 1, during step 17, the depth of the flow matches the obstacle' s height, and the discharge occurs only through the sides of the structure.

The timeline and recorded impact mechanism among the present two models are identical. However, model 1 captures the soil material overflowing the obstacle which leads to reducing the peak impact force and moderately accelerating the discharge of the soil accumulated at the front of the barrier. The effect of the discharging rate is expressed in Figure 5 as variability in the post-peak inclination of the curves and the obtained magnitude of forces. The post-peak segment of the curve attributed to model 1, shows a steeper inclination and lower value of induced soil forces, associated with the deposit at the front of the obstacle, compared to model 2. The obtained peak forces from the present analyses are higher than the corresponding value reported in the simulations for the full-spanning width obstacle, owing to the latter's efficiency in reducing the kinematics of the flow and transforming the kinetic into potential energy. In the present analyses, the obstacles do not obstruct the flow and therefore, the granular material impacts the element with increased velocity.

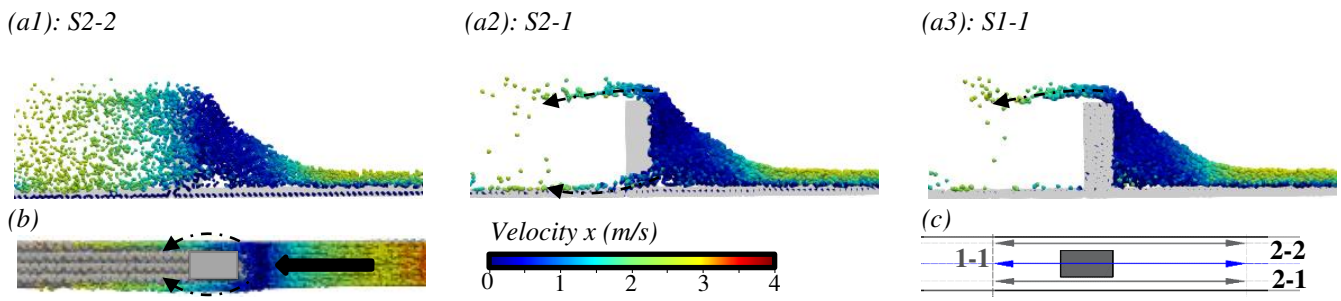

Figure 6: Analysis results: ***(a1, a2, a3) Step 14:*** *Side view along flume sections,* ***(b) Step 11:*** *Top view;* ***(c)*** *Section-cuts*

Finally, the residual forces from the present analyses show reduced magnitude compared to the initial model owing to the modified blockage ratio which results in limiting the deposit at the face of the obstacle.

4 CONCLUSIONS

This study presents the variability in the impact mechanism and recorded earth pressures induced to a structure with reduced dimensions, compared to the width of a dry granular flow. For this purpose, an experimental flume test from the literature was simulated, in accordance with the numerical assumptions suggested by Cuomo et al. (2021), that calibrated their 2D MPM model upon the same test. Initially, a 2D model was developed and validated against the results of the considered study. To account for the modified obstacle's dimensions the model was extended to the 3D domain. The required number of MPs was tested, while accounting for a full-width obstacle, to obtain comparable results with the reference experiment and the numerical study. To ensure the stability of the numerical solution and obtain appropriate observations with regards to the propagation of the granular flow, the developed 3D model considered 4 MPs to simulate the granular material.

The geometry of the obstacle was then, modified to induce a 50% blockage ratio to the granular flow. The interaction of the soil flow with the structure led to the development of complicated streamlines to discharge the material past the element. The recorded impact force showed a steep increase to the peak value, which then, gradually decreased owing to reducing the velocity and depth of the soil flow. The results are in agreement with the experimental observations of Zanuttigh & Lamberti (2006), who investigated the impact forces on various types of structures. The peak impact was overestimated in comparison with the corresponding value obtained from the 3D simulation for a full-width obstacle, due to the latter's ability to limit the dynamics of the incoming flow. Additional analysis is required to investigate the variability in the induced earth pressures to a structure upon different blockage ratios and slope angles, and potentially establish a methodology to quantify the corresponding loads.

5 ACKNOWLEDGEMENTS

All simulations conducted in this study deploy the open-source software Anura3D (www.mpm-dredge.eu). This work is part of a PhD study, funded from the UCL-GRS scholarship.

6 REFERENCES

Cuomo, S., Di Perna, A., & Martinelli, M. (2021). Material point method (Mpm) hydro-mechanical modelling of flows impacting rigid walls. Canadian Geotechnical Journal, 58(11), 1730–1743.

D. Guha-Sapir, R. Below, & Ph. Hoyois. (2008). EM-DAT: The CRED/OFDA International Disaster Database.

Fern, J., Rohe, A., Soga, K., & Alonso, E. (Eds.). (2019). The Material Point Method for Geotechnical Engineering. CRC Press.

Iverson, R. M. (1997). The physics of debris flows. Reviews of Geophysics, 35(3), 245–296.

Jiang, Y. J., & Towhata, I. (2013). Experimental study of dry granular flow and impact behavior against a rigid retaining wall. Rock Mechanics and Rock Engineering, 46(4), 713–729.

Koo, R. C. H., Kwan, J. S. H., Ng, C. W. W., Lam, C., Choi, C. E., Song, D., & Pun, W. K. (2017). Velocity attenuation of debris flows and a new momentum-based load model for rigid barriers. Landslides, 14(2), 617–629.

Kwan, J. S. (2012). Supplementary technical guidance on design of rigid debris-resisting barriers. https://www.researchgate.net/publication/339674650

Moriguchi, S., Borja, R. I., Yashima, A., & Sawada, K. (2009). Estimating the impact force generated by granular flow on a rigid obstruction. Acta Geotechnica, 4(1), 57–71.

Nakajima, S., Abe, K., Shinoda, M., Nakamura, S., Nakamura, H., & Chigira, K. (2019). Dynamic centrifuge model tests and material point method analysis of the impact force of a sliding soil mass caused by earthquake-induced slope failure. Soils and Foundations, 59(6), 1813–1829.

Ng, C. W. W., Song, D., Choi, C. E., Liu, L. H. D., Kwan, J. S. H., Koo, R. C. H., & Pun, W. K. (2017). Impact mechanisms of granular and viscous flows on rigid and flexible barriers. Canadian Geotechnical Journal, 54(2), 188–206.

Parisi, F., & Sabella, G. (2017). Flow-type landslide fragility of reinforced concrete framed buildings. Engineering Structures, 131, 28–43.

Scheidl, C., Chiari, M., Kaitna, R., Müllegger, M., Krawtschuk, A., Zimmermann, T., & Proske, D. (2013). Analysing Debris-Flow Impact Models, Based on a Small Scale Modelling Approach. In Surveys in Geophysics (Vol. 34, Issue 1, pp. 121–140). Kluwer Academic Publishers.

Shen, W., Zhao, T., Zhao, J., Dai, F., & Zhou, G. G. D. (2018). Quantifying the impact of dry debris flow against a rigid barrier by DEM analyses. Engineering Geology, 241, 86–96.

Soga, K., Alonso, E., Yerro, A., Kumar, K., & Bandara, S. (2016). Trends in large-deformation analysis of landslide mass movements with particular emphasis on the material point method. Geotechnique, 66(3), 248–273.

Sulsky, D., Chen, Z., & Schreyer, H. L. (1994). A particle method for history-dependent materials. Computer Methods in Applied Mechanics and Engineering, 118(1–2), 179–196.

Zanuttigh, B., & Lamberti, A. (2006). Experimental analysis of the impact of dry avalanches on structures and implication for debris flows. Journal of Hydraulic Research, 44(4), 522–534.